

QCD in Infrared Region and Spontaneous Breaking of the Chiral Symmetry

Mirzayusuf Musakhanov*

National University of Uzbekistan

E-mail: musakhanov@gmail.com

The spontaneous breaking of chiral symmetry (SBCS) is one of the most important phenomena of hadron physics. It defines the properties of all the light mesons and baryons. The Chiral Perturbation Theory (ChPT) encodes QCD hadronic correlators at low-energy region in the terms the low-energy constants (LEC) – the expansion parameters on light quark current masses m and external momenta p . The LEC's can be extracted from the phenomenology or from QCD lattice calculations. On the other hand, QCD instanton vacuum/instanton liquid model provides a very natural nonperturbative explanation of the SBCS. It provides a consistent framework for description of the pions and thus may be used for evaluation of the LEC. Our aim is to calculate the vacuum properties and the LEC's within instanton vacuum model and confront with phenomenology and lattice results.

*XXI International Baldin Seminar on High Energy Physics Problems,
September 10-15, 2012
JINR, Dubna, Russia*

*Speaker.

1. Introduction

1.1 Nonperturbative QCD in Infrared Region

QCD in the chiral limit is a good approximation to the real world and left and right-handed quarks are decoupled. But the hadrons has no chiral doublets which means that the QCD vacuum breaks the chiral symmetry. One of the signals of the Spontaneous Breaking of the Chiral Symmetry (SBCS) is the presence of the nonzero chiral quark condensate, $\langle \bar{q}q \rangle \neq 0$. The understanding of SBCS is provided by Casher-Banks formula¹:

$$\langle \bar{q}q \rangle = -\frac{\pi}{V} v(\lambda = 0), \quad (1.1)$$

The chiral condensate is thus proportional to the averaged spectral density of the QCD Dirac operator ($i\hat{\partial} + g\hat{A}$) at zero eigenvalues $v(\lambda = 0)$ [1, 2]. The key moment is that the Dirac operator in the background of topologically nontrivial field may has an exact zero modes with $\lambda = 0$ and in an accordance with a general Atiah–Singer index theorem the number of these modes equal to Pontryagin index or the topological charge of the background field. Then, the SBCS is due to of a delocalization of the would-be zero modes, induced by the background of a vacuum topologically nontrivial fields, resulting from quarks hopping between them. On the other hand the QCD sum rules phenomenology requests that the QCD vacuum has the gluon condensate [3]:

$$\frac{1}{32\pi^2} \langle G_{\mu\nu}^a G_{\mu\nu}^a \rangle \simeq (200 \text{ MeV})^4. \quad (1.2)$$

The simplest way to explain both phenomena – the chiral quark condensate and the gluon condensate is the instanton vacuum/instanton liquid model (see reviews [1, 2]). In the model the gluon condensate is directly related to the instanton density as $\frac{1}{32\pi^2} \langle G_{\mu\nu}^a G_{\mu\nu}^a \rangle = N/V = \bar{R}^{-4}$, where from Eq.(1.2) the average inter-instanton distance in Euclidian space $\bar{R} \simeq (200 \text{ MeV})^{-1} = 1 \text{ fm}$. With this value for \bar{R} and phenomenological value for the quark condensate $\langle \bar{q}q \rangle \simeq -(250 \text{ MeV})^3$ the average size of the instanton is estimated as $\bar{\rho} \simeq 0.33 \text{ fm}$.

The main problem of the instanton vacuum model is the lack of the confinement. A generalizations of the model providing the confinement was proposed recently with the price of the introducing of the other topological objects. Among them are calorons with non-trivial holonomy, BPS monopoles or dyons, vortices, etc..

1.2 Lattice QCD in Infrared Region

In the recent decades QCD vacuum have been intensively studied by direct numerical simulations on the lattice. The presence of non-trivial topological objects was demonstrated by using various configuration-smoothing methods. The typical view of the distributions of the action and topological charge density before and after few steps of the “cooling” was the following: before “cooling” they are heavily dominated by perturbative zero-point fluctuations of the gluon fields. The “cooling” suppresses these fluctuations which leads to a smooth background coinciding with an ensemble of instantons and antiinstantons with $\bar{\rho} \simeq 0.36 \text{ fm}$ and $\bar{R} \simeq 0.89 \text{ fm}$ [4].

¹ Assumed thermodynamic limit means that the volume V goes to infinity faster than quark mass m goes to zero.

But recently the QCD instanton vacuum model was challenged by the detailed lattice studies of topological charge density distribution by means of overlap Dirac operator (possess an exact chiral symmetry on the lattice) which shows a three-dimensional, laminar and highly singular structure which seems contradict the instanton and similar pictures [5]. Probably the structure of the QCD vacuum much more rich and we have to add another topological objects mentioned above.

The question: which component of QCD vacuum is most important for the SBCS? The answer is given by the comparison of the momentum dependence of the dynamical quark mass $M(q)$ in the chiral limit given at instanton vacuum model and lattice QCD, Fig.1. Model q -dependence of $M(q)$ is mostly due to the quark zero-mode function in the (anti)instanton field. We see very good coincidence **without any fitting** of the lattice results with the model.

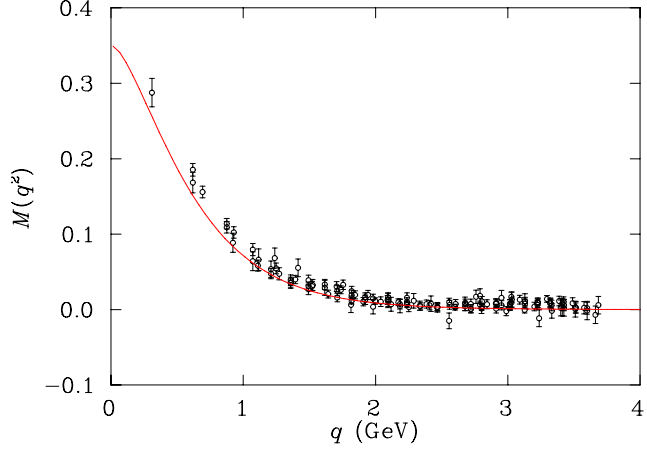


Figure 1: Momentum dependence of dynamical quark mass $M(q)$ in the chiral limit. Points: lattice result [6]. Red line: instanton vacuum model [7], **no fitting**.

The details of the instanton size distribution extracted from lattice simulations of the instanton liquid are presented at the Fig.2.

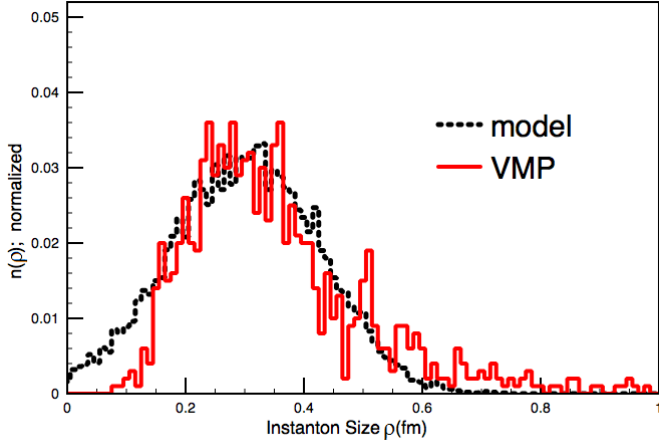


Figure 2: $n_{model}(\rho) \propto \exp \left[-\frac{(\rho - \bar{\rho})^2}{2\sigma^2} \right]$, with $\bar{\rho} = 0.3$ fm, $\sigma = 0.13$ fm, $\bar{R} \simeq 1.07$ fm and the VMP distribution from the corresponding lattice configurations [8].

1.3 QCD vacuum and pion physics

The properties of the QCD vacuum and its lowest excitations—pions are encoded in Low-Energy Constants (LEC) of Chiral Perturbation Theory (ChPT). It is natural to confront LEC's derived from the model with the phenomenology and lattice calculations of them. ChPT gives the correlators in terms of LEC's as coefficients in the expansion over the current quark mass m and external momentum of the order of M_π (taking into account that in the lowest order $m_\pi^2 \sim m$). This expansion have to take into account a chiral log terms $\sim \log m_\pi^2$ due to the contribution of the pion loops. $N_f = 2$ lowest q^2 order effective lagrangian L_2 have two LEC's F and B . They correspond to the observables: F – the pion decay constant in the chiral limit and $m_\pi^2 = 2Bm$ – the pion mass square in the lowest order on m [9]. At q^4 order effective lagrangian L_4 has 10 independent *bare* LEC's l_i, h_i . They are renormalized by pion loops to \bar{l}_i . Physical observables should be expressed in terms of \bar{l}_i [9].

Our aim is to calculate the vacuum properties and the LEC's within instanton vacuum model and compare with phenomenology and lattice results.

2. Instanton vacuum model

Instanton A^I (antiinstanton $A^{\bar{I}}$) is a solution of Yang-Mills equations in Euclidian space with topological charge $= 1(-1)$ and correspond to the tunneling process of the gluon fields. Instanton collective coordinates are 4 (*centre*) $+ 1$ (*size*) $+ (4N_c - 5)$ (*orientations*) $= 4N_c$. It is assumed that vacuum background is given by $A = \sum_I A^I + \sum_{\bar{I}} A^{\bar{I}}$. The main parameters of the instanton vacuum are average interinstanton distance \bar{R} and average size $\bar{\rho}$. The estimates of them are the following: lattice estimates: $\bar{R} \approx 0.89 \text{ fm}$, $\bar{\rho} \approx 0.36 \text{ fm}$ [4], phenomenological estimates: $\bar{R} \approx 1 \text{ fm}$, $\bar{\rho} \approx 0.33 \text{ fm}$ [1], our estimate (corresponding ChPT $F_{\pi, m=0} = 88 \text{ MeV}$, $\langle \bar{q}q \rangle_{m=0} = -(255 \text{ MeV})^3$): $\bar{R} \approx 0.76 \text{ fm}$, $\bar{\rho} \approx 0.32 \text{ fm}$. Thus within $10 - 15\%$ uncertainty different approaches give similar estimates. We see that the packing parameter $\pi^2 (\bar{\rho}/\bar{R})^4 \sim 0.1$ is small and independent averaging over instanton positions and orientations is justified.

2.1 Light quarks in the instanton vacuum

We have to calculate the correlators beyond the chiral limit to extract LEC's. Our starting point is the interpolation formula [10, 11, 12, 13, 14] for the quark propagator in the field of single instanton:

$$S_i = S_0 - S_0 \hat{p} \frac{|\Phi_{0i}\rangle \langle \Phi_{0i}|}{\langle \Phi_{0i} | \hat{p} S_0 \hat{p} | \Phi_{0i} \rangle} \hat{p} S_0, \quad S_0 = \frac{1}{\hat{p} + im}, \quad (i\hat{\partial} + g\hat{A}_i)\Phi_{0i} = 0 \quad (2.1)$$

where Φ_{0i} is the quark zero-mode function. The advantage of the formula shown by the projection of the propagator to the zero-mode

$$S_i |\Phi_{0i}\rangle = \frac{1}{im} |\Phi_{0i}\rangle, \quad \langle \Phi_{0i} | S_i = \langle \Phi_{0i} | \frac{1}{im}. \quad (2.2)$$

as it must be. Also, the calculations of the single-instanton quark effective action reproduce exactly most important for our problems the $(m\rho)^2 \ln m\rho$ -term from [15].

On the other hand the interpolation formula provide the summing up the re-scattering series for the full propagator (in the presence also of the flavor external fields $\hat{V} = s + p\gamma_5 + \hat{v} + \hat{a}\gamma_5$):

$$\begin{aligned} \tilde{S} - \tilde{S}_0 &= -\tilde{S}_0 \sum_{i,j} \hat{p} |\phi_{0i}\rangle \left\langle \phi_{0i} \left| \left(\frac{1}{\hat{p}\tilde{S}_0\hat{p}} \right) \right| \phi_{0j} \right\rangle \langle \phi_{0j} | \hat{p} \tilde{S}_0, \\ |\phi_0\rangle &= \frac{1}{\hat{p}} L \hat{p} |\Phi_0\rangle, \quad \tilde{S}_0 = \frac{1}{\hat{p} + \hat{V} + im}, \quad L_i(x, z_i) = \text{Pexp} \left(i \int_{z_i}^x dy_\mu (v_\mu(y) + a_\mu(y)\gamma_5) \right). \end{aligned} \quad (2.3)$$

Gauge connections L_i provide flavor gauge-covariance of the propagator \tilde{S} .

Let's represent the quark determinant as $\text{Det} = \text{Det}_{high} \times \text{Det}_{low}$ [7]. The high-frequencies part of the quark determinant Det_{high} can be calculated in single-instanton approximation, while the low-frequencies part Det_{low} get the contribution from the whole set of the instantons according the formula:

$$\ln \tilde{\text{Det}}_{low} = \text{Tr} \int_m^{\bar{M}} dm' \tilde{S}(m') = \ln \det \langle \phi_{0,i} | \hat{p} \tilde{S}_0^{fg} \hat{p} | \phi_{0,j} \rangle, \quad (2.4)$$

The partition function for the light quarks $Z_N[V]$ is given by the averaging of $\tilde{\text{Det}}_{low}$ over instantons collective coordinates. It was done by means of the fermionization with constituent quarks ψ^\dagger, ψ and leads to the t'Hooft-like nonlocal quark interaction term Y_{N_f} with $2N_f$ legs [10, 11]. In the following we consider the $N_f = 2$ case, neglecting the influence of strange and heavier quarks for the pion physics observables.

Further exponentiation in $Z_N[V]$ introduce the integration over dynamical couplings λ_\pm and we have the partition function in the form:

$$\begin{aligned} Z_N[V] &= \int d\lambda_+ d\lambda_- D\psi^\dagger D\psi e^{-S}, \\ S &= \psi^\dagger (i\hat{\partial} + \hat{V} + im) \psi + \sum_{\pm} \left(N_\pm \ln \frac{K}{\lambda_\pm} - N_\pm + \lambda_\pm Y_2^\pm \right), \\ Y_2^\pm &= \int d\rho n(\rho) \left(\alpha^2 \det_f J^\pm + \beta^2 \det_f J_{\mu\nu}^\pm \right), \quad \alpha^2 = \frac{2N_c - 1}{(N_c^2 - 1)2N_c}, \quad \beta^2 = \frac{\alpha^2}{8N_c - 4}, \\ J_{fg}^\pm &= (2\pi\rho)^2 \psi_f^\dagger \bar{L} F \frac{1 \pm \gamma_5}{2} F L \psi_g, \quad J_{\mu\nu,fg}^\pm = (2\pi\rho)^2 \psi_f^\dagger \bar{L} F \sigma_{\mu\nu} \frac{1 \pm \gamma_5}{2} F L \psi_g, \quad \bar{L} = \gamma_4 L^\dagger \gamma_4. \end{aligned} \quad (2.5)$$

The interaction term non-locality form-factor F in the momentum space is completely defined by Fourier-transform of the quark zero-mode function as:

$$F(k) = -\frac{d}{dt} [I_0(t)K_0(t) - I_1(t)K_1(t)]_{t=\frac{|k|\rho}{2}} \approx \frac{1}{1 + 2(|k|\rho)^2}, \quad |k|\rho < 3; \quad \frac{\sqrt{2}}{(|k|\rho)^3}, \quad |k|\rho > 3. \quad (2.6)$$

So, the range of the non-locality is given by the instanton size ρ , as was expected.

The main purpose of our work is the calculations of various correlators with account of the $\mathcal{O}(1/N_c, m, m/N_c, m/N_c \ln m)$ -corrections, which means double expansion over $1/N_c$ and m . We estimated such NLO corrections [12, 13, 14, 16]:

1. The width of the instanton size distribution is $\mathcal{O}(1/N_c)$. We found that the finite width corrections are negligible, as were expected. For example, the account of the finite width parameter σ (see $n_{model}(\rho)$ from the Fig.2) lead to the corrections $\approx 2.6\%$ for $\langle \bar{q}q \rangle$ and $\approx 5\%$ for F_π^2 .

2. The back-reaction of the light quark determinants to the instanton vacuum properties does not sizably change the distribution over $N_+ + N_-$ but radically change the distribution over $N_+ - N_-$. Any $m_f = 0$ leads to δ -function type of the latter distribution. In the following we take $N_+ = N_-$.
3. There are the quark-quark tensor interaction terms which are $1/N_c$ -suppressed and thus are absent in the LO. It might give the contribution to the vacuum magnetic susceptibility χ . Our estimate shows that it leads to the correction $\leq 1\%$ to the χ , which is certainly negligible.
4. We found the importance of the meson loops contribution. And most important among them are pion loops, certainly. They lead to the chiral logs and numerically large corrections.

Though the evaluation of the meson loop corrections in the instanton vacuum model is similar to the earlier meson loop evaluations in the NJL model [17, 18, 19, 20] important differences should be mentioned:

1. Due to nonlocal formfactors there is no need to introduce independent fermion and boson cutoffs Λ_f, Λ_b . The natural cutoff scale for all the loops (including meson loops) is the inverse instanton size ρ^{-1} .
2. In the instanton vacuum model the quark coupling constant λ is defined through the saddle-point equation whereas it is a fixed external parameter in NJL.

3. Vacuum properties

First it were calculated the dependencies of the dynamical quark mass M and the quark condensate $\langle\bar{q}q\rangle$ (in GeV^3) as a functions of current mass m (in GeV) [12], see Fig. 3.

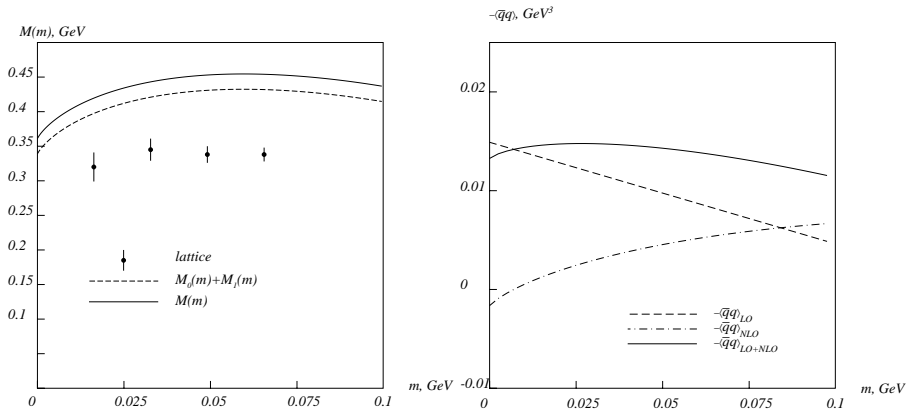


Figure 3: Left panel: m -dependence of the dynamical quark mass M on the scale $\bar{\rho}^{-1} \approx 0.6 GeV$. The solid curve – the exact numerical solution Eq. (3.1). The dashed curve – the solution obtained by the $1/N_c$ iterations with the same accuracy. Lattice data points are from [21], where the scale is $1.64 GeV$.

Right panel: m -dependence of the quark condensate $-\langle\bar{q}q\rangle$ Eq. (3.2). The long-dashed curve is the LO result, the short-dashed curve is the NLO contribution, the solid curve is the total one. The dot-dashed line is the leading-order in $1/N_c$ -expansion.

We found

$$M(m) = 0.36 - 2.36m - \frac{m}{N_c}(0.808 + 4.197 \ln m) + \mathcal{O}\left(m^2, \frac{1}{N_c}\right), \quad (3.1)$$

and

$$-\langle \bar{q}q \rangle(m) = (0.00497 - 0.034m)N_c + (0.00168 - 0.049m - 0.058m \ln m) + \mathcal{O}\left(m^2, \frac{1}{N_c^2}\right) \quad (3.2)$$

We see a very essential contributions of the chiral logs to the m dependencies of $M(m)$ and $\langle \bar{q}q \rangle(m)$. They are coming from the pion loops, certainly.

3.1 Vacuum magnetic susceptibility

External electromagnetic field $F_{\mu\nu}$ generate the quark currents in the QCD vacuum, described by the magnetic susceptibility $\chi_f(m_f)$:

$$\langle 0 | \psi_f^\dagger \sigma_{\mu\nu} \psi_f | 0 \rangle_F = e_f \chi_f(m_f) \langle i \psi^\dagger \psi \rangle_0 F_{\mu\nu} \quad (3.3)$$

Here $\langle i \psi^\dagger \psi \rangle_0 = -\langle \bar{q}q \rangle(m=0)$ is a normalization factor. QCD sum rules estimate [22, 23] gives: $\chi_f(m_f) \langle i \psi^\dagger \psi \rangle_0 \sim 40 - 70 \text{ MeV}$. The magnetic susceptibility is measurable in jet production at $q_\perp \gg \Lambda_{QCD}$ at the process $\gamma + N \rightarrow (\bar{q}q) + N$ with polarized photon [24].

Our result for $\chi(m) \langle i \psi^\dagger \psi \rangle_0$ [14] with the accuracy $\mathcal{O}\left(m^2, \frac{1}{N_c^2}\right)$ is

$$\chi(m) \langle i \psi^\dagger \psi \rangle_0 = N_c \left(0.015 + 5 \cdot 10^{-4}m + \frac{m}{2\pi^2} \ln m \right) - 0.007 - 0.415m - 0.198m \ln m. \quad (3.4)$$

Last term here is in correspondence with the newly established chiral log theorem:

$$\chi(m) = \chi(0) \left(1 - \frac{3m_\pi^2}{32\pi^2 F^2} \ln m_\pi^2 \right) \quad (3.5)$$

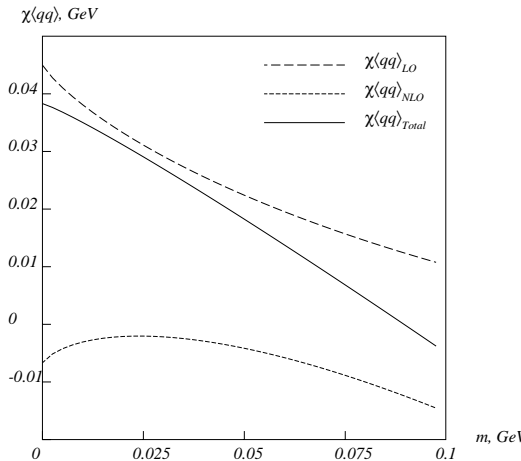


Figure 4: Magnetic susceptibility $\chi(m) \langle i \psi^\dagger \psi \rangle_0$ as a function of current quark mass m .

We see that the strange quark contribution to the magnetic susceptibility is much less than lightest quarks one, Fig. 4. This result might be important for the phenomenology of the process $\gamma + N \rightarrow (\bar{q}q) + N$ mentioned above.

4. Pion properties and low-energy constants \bar{l}_3, \bar{l}_4

We calculated the two-point axial-isovector currents correlator [14]:

$$\int d^4x e^{-iq\cdot x} \langle j_\mu^{A,i}(x) j_\nu^{A,j}(0) \rangle = \delta_{ij} F_\pi^2 \left(\delta_{\mu\nu} - \frac{q_\mu q_\nu}{q^2 + M_\pi^2} \right) + \mathcal{O}(q^2) \quad (4.1)$$

Here M_π has a meaning of pion mass and F_π – pion decay constant.

We found

$$\begin{aligned} F_\pi^2 &= N_c \left(\left(2.85 - \frac{0.869}{N_c} \right) - \left(3.51 + \frac{0.815}{N_c} \right) m - \frac{44.25}{N_c} m \ln m + \mathcal{O}(m^2) \right) \cdot 10^{-3} [GeV^2] \\ M_\pi^2 &= m \left(\left(3.49 + \frac{1.63}{N_c} \right) + m \left(15.5 + \frac{18.25}{N_c} + \frac{13.5577}{N_c} \ln m \right) + \mathcal{O}(m^2) \right) [GeV^2] \end{aligned} \quad (4.2)$$

represented by Fig.5.

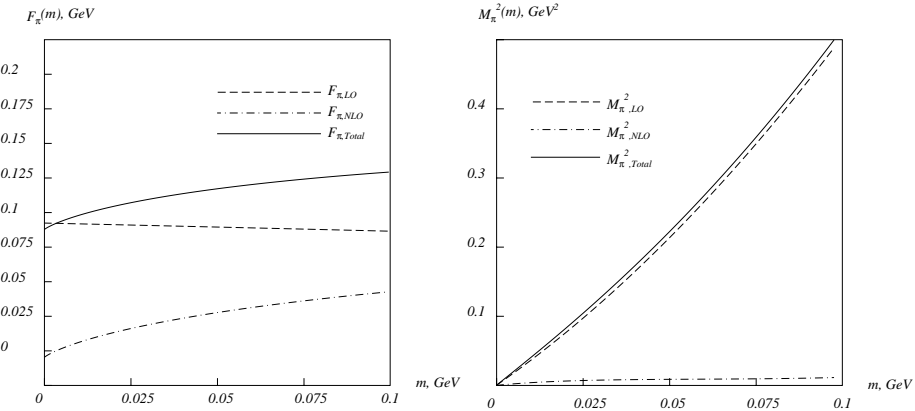


Figure 5: Left panel: m -dependence of the pion decay constant F_π . The long-dashed curve is the LO contribution, the short-dashed curve is the NLO contribution, the solid curve is the total LO+NLO contribution. The dot-dashed line represents the leading-order in $1/N_c$ -expansion result, evaluated with the mass M_0 . Right panel: m -dependence of the pion mass M_π . The long-dashed curve is the LO contribution, the short-dashed curve is the NLO contribution, the solid curve is the total LO+NLO contribution. The dot-dashed line represents the leading-order in $1/N_c$ -expansion result, evaluated with the mass M_0 .

According to [9], the low-energy constants \bar{l}_3, \bar{l}_4 of the chiral lagrangian may be extracted from the $\mathcal{O}(m)$ -corrections to physical quantities, e.g.

$$M_\pi^2 = m_\pi^2 \left(1 - \frac{m_\pi^2}{32\pi^2 F^2} \bar{l}_3 + \mathcal{O}(m_\pi^4) \right) \quad (4.3)$$

$$F_\pi^2 = F^2 \left(1 + \frac{m_\pi^2}{8\pi^2 F^2} \bar{l}_4 + \mathcal{O}(m_\pi^4) \right). \quad (4.4)$$

Here $m_\pi^2 = 2mB$. Lowest order LEC's $B = 2.019 \text{ GeV}$ and $F = 88 \text{ MeV}$ were taken as an input to fix main instanton vacuum parameters as $\bar{\rho} = 0.350 \text{ fm}$ and $\bar{R} = 0.856 \text{ fm}$.

Then, we found (neglecting by the terms $\mathcal{O}\left(\frac{1}{N_c}\right)$)

$$\bar{l}_3 = -1.1425N_c + 0.0738 - 0.999 \ln m, \quad \bar{l}_4 = -0.0793N_c + 0.01876 - \ln m, \quad (4.5)$$

which gives at $m = 0.0055 \text{ GeV}$, $\bar{l}_3 = 1.84$, $\bar{l}_4 = 4.98$ and corresponding $M_\pi = 0.142 \text{ GeV}$, $F_\pi = 0.0937 \text{ GeV}$. Our values of (\bar{l}_3, \bar{l}_4) should be compared with the phenomenological estimates [9, 25] as well as lattice predictions [26, 27, 28, 29, 30, 31, 32] given in Fig.6.

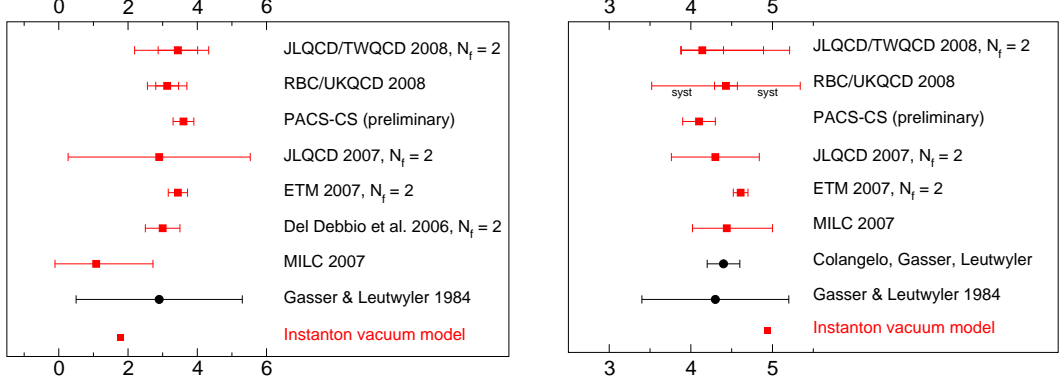


Figure 6: The LEC's \bar{l}_3 (left panel) and \bar{l}_4 (right panel) – recent lattice results from different collaborations [26, 27, 28, 29, 30, 31, 32], phenomenological estimates [9, 25] and our result.

4.1 Isospin breaking by $m_u - m_d \neq 0$ and LEC's h_3 and l_7

The correlator of the iso-vector pseudoscalar and iso-singlet pseudoscalar currents and splitting between the $\langle \bar{u}u \rangle$ and $\langle \bar{d}d \rangle$ quark condensates in QCD are proportional to $m_u - m_d$ and described by LEC's h_3 and l_7 as

$$i \int dx \langle P^3(x) P^0(0) \rangle e^{iqx} = \frac{8B^3(m_u - m_d)l_7}{q^2 - M_\pi^2} + O(q^2), \quad \langle \bar{u}u \rangle - \langle \bar{d}d \rangle = 4B^2(m_u - m_d)h_3. \quad (4.6)$$

LEC l_7 define the pion masses shift due to $m_u - m_d \neq 0$:

$$(M_{\pi_0}^2 - M_{\pi_\pm}^2) \delta_m = -(m_u - m_d)^2 \frac{2B^2}{F^2} l_7 \approx -(m_u - m_d)^2 1.2 \cdot 10^{-3} l_7. \quad (4.7)$$

Phenomenological estimate (GL, AP84) $l_7 \sim 5 \cdot 10^{-3}$. Our estimates [16] for l_7 and h_3 are

$$l_7 \approx (6.6 \pm 2.4) \cdot 10^{-4}, \quad h_3 \approx 5.48 \cdot 10^{-3}. \quad (4.8)$$

We found strong dependence of the l_7 on the instanton vacuum parameters $\bar{\rho}$ and \bar{R} . Confronting with the possible lattice calculation of this one will fix these parameters well.

5. Summary

SBCS is generated by the ‘hopping’ of quarks between topologically nontrivial gluon lumps leading to changing of quark chirality. The strong evidence in favor of the instanton vacuum model given by the momentum dependence of the dynamical quark mass $M(p)$ found in the lattice calculations (see Fig.1).

The proposed interpolation formula (2.1) for the quark propagator in the single instanton field and in the presence of the flavor external fields lead to the low-frequencies quark determinant (2.4).

Next task was a derivation of the light quarks partition function $Z[V]$, which is a functional of the external flavor fields V . For this one we averaged the quark determinant over instantons, using diluteness of the instanton media. On this way it was introduced constituent quarks as a tool of this averaging.

The partition function (2.5) has t'Hooft-like interaction terms with $2N_f$ quark legs, where the coupling λ is not a fixed one, but must be calculated from saddle-point condition. We considered $N_f = 2$ -case.

Since we are going beyond of the chiral limit we have to calculate the correlators with account of $O(1/N_c, m, m/N_c, m/N_c \ln m)$ -corrections. Within the model there are the contributions of meson loops, finite width of instanton size distribution and quark-quark tensor interactions term to these corrections. We found that the most important are meson loops, while other contributions are negligible.

ChPT describes SBCS in low-energy region in the terms of LEC's. We fixed the main parameters of the model \bar{R} and $\bar{\rho}$ in terms of lowest p^2 order LEC's B and F . With these parameters we also considered the vacuum magnetic susceptibility χ_f and its dependence on the current quark mass m_f , see Fig. 4. It might be important for the phenomenology of the jet production at the process $\gamma + N \rightarrow (\bar{q}q) + N$ with polarized photon.

At further step we calculated next p^4 order LEC's \bar{l}_3 , \bar{l}_4 , l_7 and h_3 . Most important among them are \bar{l}_3 and \bar{l}_4 , since there are available phenomenological and lattice estimates of them. We confronted our model calculation with available data and found reasonable correspondence, see Fig. 5.

This means that the instanton vacuum is applicable for understanding of the low-energy hadron physics, at least on the qualitative level.

I would like to thank Prof. Ernst-Michael Ilgenfritz for useful discussions during ISHEPP2012.

References

- [1] T. Schafer and E. V. Shuryak, Rev. Mod. Phys. **70** (1998) 323, arXiv:hep-ph/9610451.
- [2] D. Diakonov, Prog. Part. Nucl. Phys. **51**, 173 (2003), arXiv:hep-ph/0212026.
- [3] M. Shifman, A. Vainshtein and V. Zakharov, Nucl. Phys. B **147** (1979) 385.
- [4] M.-C. Chu, J. Grandy, S. Huang and J. Negele, Phys. Rev. Lett. **70** (1993) 225; *Phys. Rev.* D49 (1994) 6039; J. Negele, Nucl. Phys. Proc. Suppl. **73** (1999) 92, [hep-lat/9810053].
- [5] E.-M. Ilgenfritz, K. Koller, Y. Koma, G. Schierholz, T. Streuer, V. Weinberg, Phys. Rev. D **76** (2007) 034506, arXiv:0705.0018 [hep-lat].
- [6] P. O. Bowman, U. M. Heller, D. B. Leinweber, A. G. Williams and J. b. Zhang, Nucl. Phys. Proc. Suppl. **128** (2004) 23, arXiv:hep-lat/0403002.
- [7] D. Diakonov and V. Y. Petrov, Nucl. Phys. B **272** (1986) 457.
- [8] R. Millo, P. Faccioli, Phys. Rev. D **84** (2011) 034504.
- [9] J. Gasser and H. Leutwyler, Annals Phys. **158** (1984) 142.
- [10] M. Musakhanov, Eur. Phys. J. C **9** (1999) 235, arXiv:hep-ph/9810295.
- [11] M. Musakhanov, Nucl. Phys. A **699** (2002) 340.

- [12] H. C. Kim, M. M. Musakhanov and M. Siddikov, Phys. Lett. B **633** (2006) 701, arXiv:hep-ph/0508211.
- [13] K. Goeke, M. M. Musakhanov and M. Siddikov, Phys. Rev. D **76** (2007) 076007, arXiv:0707.1997 [hep-ph].
- [14] K. Goeke, H. -C. Kim, M. M. Musakhanov and M. Siddikov, Phys. Rev. D **76** (2007) 116007, arXiv:0708.3526 [hep-ph].
- [15] Jin Hur, Choonkyu Lee, Hyunsoo Min, Phys. Rev. D **80** (2009) 105024, arXiv:0909.5515 [hep-th].
- [16] K. Goeke, M. Musakhanov and M. Siddikov, Phys. Rev. D **81** (2010) 054029, arXiv:1002.0283 [hep-ph].
- [17] E. N. Nikolov, W. Broniowski, C. V. Christov, G. Ripka and K. Goeke, Nucl. Phys. A **608** (1996) 411, arXiv:hep-ph/9602274.
- [18] R. S. Plant and M. C. Birse, Nucl. Phys. A **703** (2002) 717, arXiv:hep-ph/0007340.
- [19] F. Pena, M. C. Nemes, A. H. Blin and B. Hiller, Braz. J. Phys. **29** (1999) 469.
- [20] M. Oertel, arXiv:hep-ph/0012224.
- [21] P. O. Bowman, private communication ($M(m)$ -dependence). See also P. O. Bowman, U. M. Heller, D. B. Leinweber, M. B. Parappilly, A. G. Williams and J. b. Zhang, Phys. Rev. D **71** (2005) 054507, arXiv:hep-lat/0501019.
- [22] B. L. Ioffe and A. V. Smilga, Nucl. Phys. B **232** (1984) 109.
- [23] V. M. Belyaev and Y. I. Kogan, Yad. Fiz. **40** (1984) 1035.
- [24] V. M. Braun, S. Gottwald, D. Y. Ivanov, A. Schäfer and L. Szymanowski, Phys. Rev. Lett. **89** (2002) 172001, arXiv:hep-ph/0206305.
- [25] G. Colangelo, J. Gasser and H. Leutwyler, Nucl. Phys. B **603** (2001) 125, arXiv:hep-ph/0103088.
- [26] Shoji Hashimoto, PoS LATTICE2008:011,2008, arXiv:0811.1257 [hep-lat].
- [27] C. Bernard *et al.* [MILC Collaboration], arXiv:0710.1118[hep - lat].
- [28] L. Del Debbio, L. Giusti, M. Luscher, R. Petronzio and N. Tantalo, JHEP **0702** (2007) 056.
- [29] B. Blossier *et al.* [ETM Collaboration], arXiv:0709.4574[hep-lat].
- [30] J. Noaki *et al.* [JLQCD Collaboration], arXiv:0710.0929[hep - lat].
- [31] C. Allton *et al.* [RBC/UKQCD Collaboration], arXiv:0804.0473 [hep-lat].
- [32] D. Kadoh *et al.* [PACS-CS Collaboration], arXiv:0710.3467[hep - lat].